Negative temperature coefficient thermistor based on Bi 3 Zn 2 Sb 3 O 14 ceramic: An oxide semiconductor at high temperature

M. A. L. Nobre and S. Lanfredi
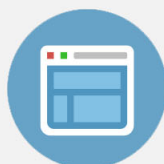
Negative temperature coefficient thermistor based on $Bi_3Zn_2Sb_3O_{14}$ ceramic: An oxide semiconductor at high temperature

M. A. L. Nobre[a)]
Faculdade de Ciências e Tecnologia-FCT, Universidade Estadual Paulista-UNESP, C.P. 467, CEP 19060-900 Presidente Prudente-SP, Brazil

S. Lanfredi[a),b)]
Faculdade de Ciências e Tecnologia-FCT, Universidade Estadual Paulista-UNESP, C.P. 467, CEP 19060-900 Presidente Prudente-SP, Brazil

$Bi_{1.5}ZnSb_{1.5}O_7$ dielectric ceramic with pyrochlore structure was investigated by impedance spectroscopy from 400 to 750 °C. Pyrochlore was synthesized by the polymeric precursor method, a chemical synthesis route derived from Pechini's method. The grain or bulk resistance exhibits a sensor temperature characteristic, being a thermistor with a negative temperature coefficient (NTC). Only a single region was identified on the resistance curve investigated. The NTC thermistor characteristic parameter (β) is equal to 7140 °C, in the temperature range investigated. The temperature coefficient of the resistance (α) was derived, being equal to -4.46×10^{-2} °C^{-1} at 400 °C. The conduction mechanism and relaxation are discussed. © *2003 American Institute of Physics.* [DOI: 10.1063/1.1566458]

Pyrochlore phase presents a general formula $A_2B_2O_7$ and spatial group $Fd_3M–O_h$ of cubic symmetry, A and B being distinct sites to be occupied by cations of several valences.[1] These materials are potentially applicable in a wide range of areas, such as catalyzing, ferromagnetics, ionic conduction, and capacitors to operate at frequencies in the gigahertz region. A specific stoichiometry with formula $Bi_{1.5}ZnSb_{1.5}O_7$ is formed in ZnO-based varistors,[2] polyphasic electroceramics, in which the microstructure depends on the precursor oxides and on their relative amounts.[3,4] These systems are typically based on ZnO and additives such as Sb_2O_3, Bi_2O_3, MnO_2, Co_2O_3, and Cr_2O_3. *A priori*, the pyrochlore does not make up the ceramic microstructure, since after its formation, it reacts with ZnO, forming $Zn_7Sb_2O_{12}$ spinel and Bi_2O_3.[3] Nevertheless, the pyrochlore can be retained.[5] Little physical information is available on $Bi_{1.5}ZnSb_{1.5}O_7$, particularly on its electric characteristic.[6,7]

This work presents a negative temperature coefficient (NTC) thermistor ceramic for high temperature based on $Bi_{1.5}ZnSb_{1.5}O_7$ pyrochlore. It is interesting to note that NTC thermistors are commonly spinels with a further combination of cations of transition metals or single cation phase. An insight is presented here for the grain features of the $Bi_{1.5}ZnSb_{1.5}O_7$ pyrochlore. The cubic single-phase $Bi_{1.5}ZnSb_{1.5}O_7$ was synthesized by chemical route based on the polymeric precursor method.[6,7] The starting reagents for preparing of pyrochlore powders were zinc acetate, citric acid, ethylene glycol, antimony oxide, and bismuth oxide. Crystalline powders were obtained by calcinations of precursor at 900 °C for 1 h. Pellet of $Bi_{1.5}ZnSb_{1.5}O_7$ was sintered via constant heating rate process in a dilatometer up to 1250 °C using a constant heating rate of 10 °C/min. A rela-tive density of 97% of the theoretical density was reached. Electrical measurements were carried out on the 8×5-mm cylindrical sample. Platinum electrodes were deposited on both faces of the sample by a platinum paste coating (Demetron 308A), which was dried at 800 °C for 30 min.

The measurements were performed in the frequency range from 5 Hz to 13 MHz, using a Solartron 1260 impedance analyzer controlled by a personal computer. A 500-mV ac signal was applied. A sample holder with a two-electrode configuration was used. The ac measurements were taken from 400 to 750 °C in 50-°C steps. A 30-min interval was used prior to the thermal and properties stabilization after each measuring. The impedance data $[Z^*(\omega)]$ were plotted in the complex plane, a plot of the real component $[Z'(\omega)]$ versus the imaginary component $[Z''(\omega)]$. $Z^*(\omega)$ is represented by equation $Z^*(\omega) = Z'(\omega) + jZ''(\omega) = Z_g^*(\omega) + Z_{gb}^*(\omega)$, where g stands for grain and gb for grain boundary. The data were analyzed by Boukamp's EQUIVCRT software. This program works in an environment developed for equivalent electric circuits, based on the fitting of the immitance spectra data.[8]

Figure 1 shows the impedance diagram of $Bi_{1.5}ZnSb_{1.5}O_7$ obtained at 450 °C. The points on the diagram are the experimental data, while the continuous line represents the theoretical adjust. An excellent agreement between the data and fitting curve is obtained. An inspection of the semicircle shows that there is a depression degree instead of a semicircle centered on the x axis. This behavior of the electrical response obeys Cole–Cole's formalism.[9] Furthermore, the shape of the diagram suggests that the electrical response is composed of at least two semicircles. Thus, in Fig. 1, the electric properties of $Bi_{1.5}ZnSb_{1.5}O_7$ can be represented by two parallel RC-equivalent circuits in series. The contribution positioned at low frequencies, $< 10^3$ Hz, corresponds to the grain boundary response. In the high-frequency range ($> 10^3$ Hz), the one corresponds to a specific property

---

[a)]Member of the UNESP/CVMat-Virtual Center of Research in Materials.
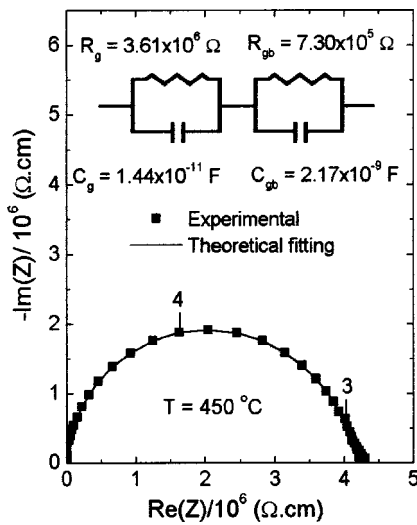[b)]Author to whom correspondence should be addressed, e-mail: silvania@prudente.unesp.br

FIG. 1. Experimental and theoretical curves of $Bi_{1.5}ZnSb_{1.5}O_7$ with corresponding equivalent circuit obtained at 450 °C. Numbers 3 and 4 give the $\log_{10}$ (signal frequency) for the corresponding point.

FIG. 2. Grain resistance, total resistance, and relaxation time as a function of temperature.

of the bulk. The depression of the semicircles is considered further evidence of a polarization phenomenon with a distribution of relaxation times. Taking into account Boukamp's formalism, the ideal character of the polarization phenomenon is represented by the Q parameter.

In this way, Q represents a nonideal capacitance that is physically determined by the parameters Y_o, with exponent n being $n \leq 1$. Y_o tends to an ideal capacitance (C), when the exponent n tends to value of 1. The departure from ideal character exhibited by the parameter Q is exclusively due the distribution of relaxation times, which leads to the decentralization phenomenon of the semicircle.[6,7,10,11] The relaxation time τ is determined by relaxation $\tau = RC$, where R is the resistance. This formalism has been successfully applied to investigation of some fundamental electric and dielectric properties of $Bi_{1.5}ZnSb_{1.5}O_7$[6,7] and $Zn_7Sb_2O_{12}$.[11,12]

Figure 2 shows grain resistance, total resistance ($R_g + R_{gb}$) and relaxation time of $Bi_{1.5}ZnSb_{1.5}O_7$ as a function of temperature. The total resistance values exhibit similar magnitudes to the grain resistance. This finding indicates that the grain boundary contribution is very small, as can be observed in Fig. 1. The evolution of the grain resistance, total resistance, and relaxation time is further characteristic of a NTC material. This behavior indicates that the conduction mechanism actuating on the grain is of the hopping type,[12] in accordance with the NTC behavior observed. The intrinsic defect of $Bi_{1.5}ZnSb_{1.5}O_7$ phase might be Sb^{3+} and/or electron holes. As a matter of fact, in addition to valence state 5,[13] the existence of cations with valences equal to 3 has been suggested.[14] The quasichemical reaction $2Sb^{4+} \rightarrow Sb^{3+} + Sb^{5+}$ has been recently hypothesized to modeling in a qualitative way the electric conductivity in $Zn_7Sb_2O_{12}$ antimoniate spinel, which provides support to the hypothesis of hopping conduction.[11,12] Similar to antimoniates pyrochlores,[14] the valence equal to 3+ has been reported at $Zn_7Sb_2O_{12}$.[15]

The relation between resistance and temperature for a negative temperature coefficient thermistor is expressed by the following equation:
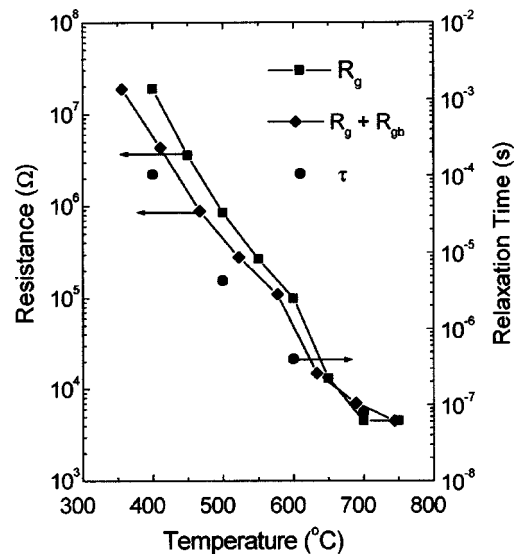
$$R_T = R_N \exp^{\beta(1/T - 1/T_N)}, \tag{1}$$

where R_T is the resistance at temperature T, R_N is the resistance at temperature T_N known, and β is a thermistor characteristic parameter. Rewriting and rearranging the terms of Eq. (1), β can be derived as follows:

$$\beta = [TT_N/(T_N - T)]\ln(R_T/R_N). \tag{2}$$

The thermistor sensitivity is defined by the temperature coefficient of resistance α, which can be expressed as a function of the β parameter, in according to following equation:

$$\alpha = (1/R)[d(R)/dT] = -\beta/T^2. \tag{3}$$

Considering R versus T curves (Fig. 2), the β parameter was calculated by Eq. (2). The β value calculated in the temperature range from 400 to 750 °C is equal to 7140 °C. The α parameter derived at 400 °C is equal to -4.46×10^{-2} °C^{-1}.

An alternative approach to analysis the impedance data is to use the electric modulus $M^*(\omega)$ represented by the equation $M^*(\omega) = j\omega C_o Z^*(\omega)$, where $j = \sqrt{-1}$ and C_o is the vacuum capacitance of the cell. This formalism is particularly suitable to detect phenomena as electrode polarization and bulk phenomenon property as apparent conductivity relaxation times. Figure 3 shows $M''(\omega)$ as a function of logarithmic frequency at several temperatures. The $M''(\omega)$ curves show only a peak at high frequency and it tends to zero at low frequencies.

Figure 4 shows the variation of normalized parameters $\tan\delta/\tan\delta_{max}$, M''/M''_{max}, and Z''/Z''_{max} as a function of logarithmic frequency measured at 500 °C. The peak frequency in M''/M''_{max} curve is slight shifted to more high-frequency region with relation to one in Z''/Z''_{max}. Through these representations, it is possible to analyze the apparent polarization by inspection of the magnitude of mismatch between the peaks of both parameters.[16] The almost overlapping of peaks of Z''/Z''_{max} and M''/M''_{max} is further evidence of a long-range conductivity. However, the feature of these three functions should be considered simultaneously prior to a precise discerning between localized and nonlocalized conduction.[16]
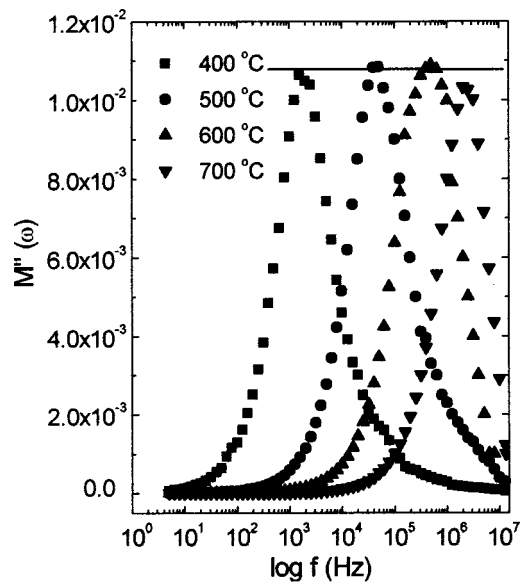
FIG. 3. $M''(\omega)$ as a function of logarithmic frequency measured at several temperatures.

Therefore, the observed polarization process is due to a localized conduction. It should be pointed out that the assignment is unequivocal to the grain or bulk.

The relaxation time is a thermally activated process. The logarithmic of relaxation times, derived from Z'' and M'' functions, as a function of reciprocal temperature $1/T$, are shown in Fig. 5. The derived data are described by Arrhenius's law:

$$\tau_g = \tau_o \exp(E_{a\tau}/kT), \qquad (4)$$

where τ_o is the pre-exponential factor or characteristic relaxation time constant and $E_{a\tau}$ is the activation energy for the conduction relaxation. Similar values for $E_{a\tau Z''}$ and $E_{a\tau M''}$ are observed on the entire range of temperature measurements, being equal to 1.38 and 1.37 eV, respectively. These
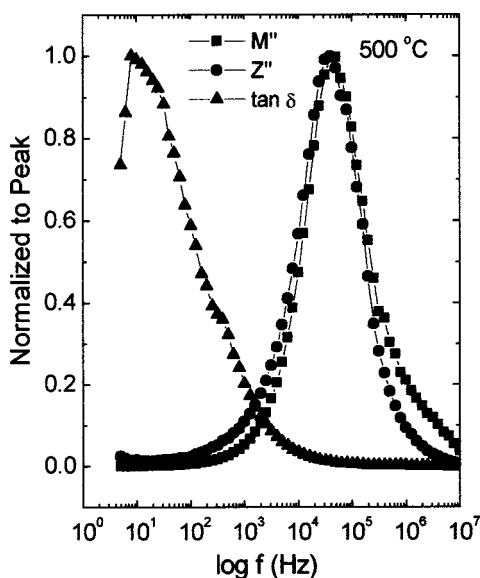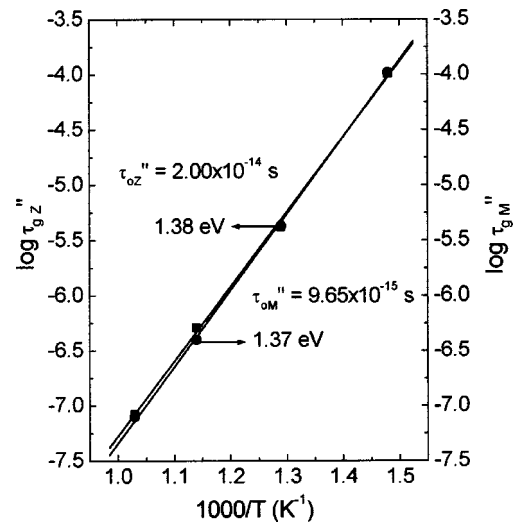

FIG. 5. Arrhenius diagram of relaxation times $\tau_{Z''}$ and $\tau_{M''}$ as a function of reciprocal temperature $1/T$.

values are equal. τ_o values are of the order of 10^{13} Hz, compatible with the defect lattice vibration frequency. Therefore, the relaxation phenomenon of grain stems from the lattice-defect structure. Dipole relaxation can be discarded, suggesting that vacancy oxygen is not an intrinsic defect.

As a whole, in ZnO-based varistor, the secondary phases as spinels and pyrochlore antimoniates occupy specific regions of the microstructure.[17] These regions might be composed of distinct phases, with stoichiometry close to Bi_2O_3, $Zn_7Sb_2O_{12}$, and $Bi_{1.5}ZnSb_{1.5}O_7$.[17] At the moment, both $Zn_7Sb_2O_{12}$[11,12] and $Bi_{1.5}ZnSb_{1.5}O_7$ are NTC thermistors, depending on the processing. Under temperature effect, the regions containing NTC thermistors undergo an enhancement of the effect of draining of the current. This current leads to heating that in turn leads to further current. This might explain the continuous production of localized density current, which gives rise to further insight on some intriguing component failures, for example, the puncture failure.[17]

FIG. 4. Normalized tan δ, normalized imaginary part of the impedance (Z''), and normalized imaginary part of the modulus (M'') as a function of frequency for $Bi_{1.5}ZnSb_{1.5}O_7$ at 500 °C.

[1] S. L. Patil and V. S. Darshane, Indian J. Phys., A **A55**, 204 (1981).
[2] M. Matsuoka, Jpn. J. Appl. Phys. **10**, 736 (1971).
[3] E. R. Leite, M. A. L. Nobre, E. Longo, and J. A. Varela, *Sintering Technology* (Marcell Dekker, New York, 1996), p. 481.
[4] M. A. L. Nobre, M. R. Moraes, E. Longo, and J. A. Varela, *Sintering Science and Technology*, (The Pennsylvania State University, University Park, PA, 2000), p. 129.
[5] E. Olson and G. L. Dunlop, J. Am. Ceram. Soc. **66**, 5072 (1989).
[6] M. A. L. Nobre and S. Lanfredi, Mater. Lett. **47**, 362 (2001).
[7] M. A. L. Nobre and S. Lanfredi, J. Mater. Sci.: Mater. Electron. **13**, 235 (2002).
[8] B. A. Boukamp, Equivalent Circuit. EQUIVCRT Program—Users Manual (University of Twente-Holand, Enschede, 1989), Vol. 3, p. 97.
[9] K. S. Cole and R. H. Cole, J. Chem. Phys. **9**, 341 (1941).
[10] S. Lanfredi, J. F. Carvalho, and A. C. Hernandes, J. Appl. Phys. **88**, 283 (2000).
[11] M. A. L. Nobre and S. Lanfredi, Mater. Lett. **50**, 322 (2001).
[12] M. A. L. Nobre and S. Lanfredi, Appl. Phys. Lett. **81**, 451 (2002).
[13] D. Huiling and Y. Xi, J. Phys. Chem. Solids **63**, 2123 (2002).
[14] M. A. Subramanian, A. Clearfield, A. M. Umarje, G. K. Shenoy, and G. V. Subbarao, J. Solid State Chem. **52**, 124 (1984).
[15] S. Ezhilvalavam and T. R. N. Kutty, Appl. Phys. Lett. **68**, 2693 (1996).
[16] R. Gerhardt, J. Phys. Chem. Solids **55**, 1491 (1994).
[17] T. K. Gupta, J. Am. Ceram. Soc. **73**, 1817 (1990).